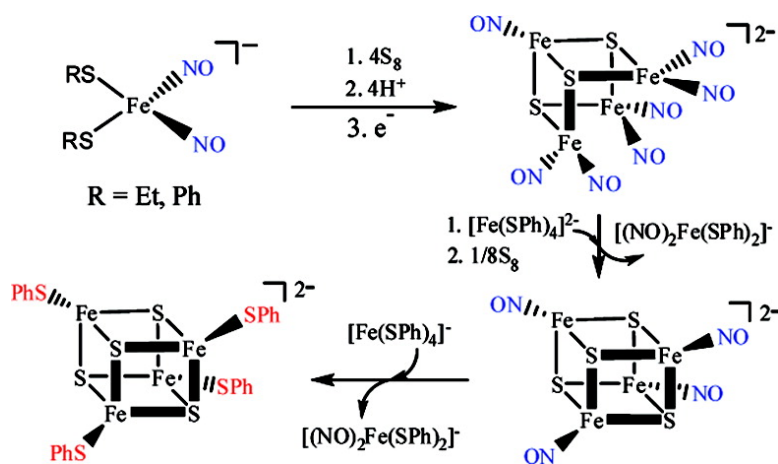


Transformation of Dinitrosyl Iron Complexes [(NO)Fe(SR)] (R = Et, Ph) into [4Fe-4S] Clusters [FeS(SPh)]: Relevance to the Repair of the Nitric Oxide-Modified Ferredoxin [4Fe-4S] Clusters

Chih-Chin Tsou, Zong-Sian Lin, Tsai-Te Lu, and Wen-Feng Liaw

J. Am. Chem. Soc., **2008**, 130 (50), 17154-17160 • DOI: 10.1021/ja806050x • Publication Date (Web): 17 November 2008

Downloaded from <http://pubs.acs.org> on February 8, 2009



More About This Article

Additional resources and features associated with this article are available within the HTML version:

- Supporting Information
- Access to high resolution figures
- Links to articles and content related to this article
- Copyright permission to reproduce figures and/or text from this article

[View the Full Text HTML](#)

Transformation of Dinitrosyl Iron Complexes $[(\text{NO})_2\text{Fe}(\text{SR})_2]^-$ (R = Et, Ph) into [4Fe-4S] Clusters $[\text{Fe}_4\text{S}_4(\text{SPh})_4]^{2-}$: Relevance to the Repair of the Nitric Oxide-Modified Ferredoxin [4Fe-4S] Clusters

Chih-Chin Tsou, Zong-Sian Lin, Tsai-Te Lu, and Wen-Feng Liaw*

Department of Chemistry, National Tsing Hua University, Hsinchu 30013, Taiwan, Republic of China

Received August 1, 2008; E-mail: wfliaw@mx.nthu.edu.tw

Abstract: Transformation of dinitrosyl iron complexes (DNICs) $[(\text{NO})_2\text{Fe}(\text{SR})_2]^-$ (R = Et, Ph) into [4Fe-4S] clusters $[\text{Fe}_4\text{S}_4(\text{SPh})_4]^{2-}$ in the presence of $[\text{Fe}(\text{SPh})_4]^{2-}$ and S-donor species S_8 via the reassembling process $[(\text{NO})_2\text{Fe}(\text{SR})_2]^- \rightarrow [\text{Fe}_4\text{S}_3(\text{NO})_7]^-$ (1)/ $[\text{Fe}_4\text{S}_3(\text{NO})_7]^{2-}$ (2) $\rightarrow [\text{Fe}_4\text{S}_4(\text{NO})_4]^{2-}$ (3) $\rightarrow [\text{Fe}_4\text{S}_4(\text{SPh})_4]^{2-}$ (5) was demonstrated. Reaction of $[(\text{NO})_2\text{Fe}(\text{SR})_2]^-$ (R = Et, Ph) with S_8 in THF, followed by the addition of HBF_4 into the mixture solution, yielded complex $[\text{Fe}_4\text{S}_3(\text{NO})_7]^-$ (1). Complex $[\text{Fe}_4\text{S}_3(\text{NO})_7]^{2-}$ (2), obtained from reduction of complex 1 by $[\text{Na}][\text{biphenyl}]$, was converted into complex $[\text{Fe}_4\text{S}_4(\text{NO})_4]^{2-}$ (3) along with byproduct $[(\text{NO})_2\text{Fe}(\text{SR})_2]^-$ via the proposed $[\text{Fe}_4\text{S}_3(\text{SPh})(\text{NO})_4]^{2-}$ intermediate upon treating complex 2 with 1.5 equiv of $[\text{Fe}(\text{SPh})_4]^{2-}$ and the subsequent addition of 1/8 equiv of S_8 in CH_3CN at ambient temperature. Complex 3 was characterized by IR, UV-vis, and single-crystal X-ray diffraction. Upon addition of complex 3 to the CH_3CN solution of $[\text{Fe}(\text{SPh})_4]^-$ in a 1:2 molar ratio at ambient temperature, the rapid NO radical-thiyl radical exchange reaction between complex 3 and the biomimetic oxidized form of rubredoxin $[\text{Fe}(\text{SPh})_4]^-$ occurred, leading to the simultaneous formation of [4Fe-4S] cluster $[\text{Fe}_4\text{S}_4(\text{SPh})_4]^{2-}$ (5) and DNIC $[(\text{NO})_2\text{Fe}(\text{SPh})_2]^-$. This result demonstrates a successful biomimetic reassembly of [4Fe-4S] cluster $[\text{Fe}_4\text{S}_4(\text{SPh})_4]^{2-}$ from NO-modified [Fe-S] clusters, relevant to the repair of DNICs derived from nitrosylation of [4Fe-4S] clusters of endonuclease III back to [4Fe-4S] clusters upon addition of ferrous ion, cysteine, and IscS.

Introduction

Nitric oxide (NO) regulates various physiological reactions including vasodilation, neuronal transmission, inflammation, immune function, and cancer killing.^{1,2} DNICs and RSNO are known to be two possible forms for storage and transport of NO in biological systems.³ DNICs are intrinsic NO-derived species that can exist in various NO-overproducing tissues. In vivo, nitric oxide can be stabilized and stored in the form of dinitrosyl iron complexes with proteins (protein-bound DNICs) and is probably released from cells in the form of low-molecular-weight dinitrosyl iron complexes (LMW-DNICs).⁴ Characterization of both protein-bound and low-molecular-weight DNICs

in vitro has been made possible via their distinctive EPR signal at $g = 2.03$.¹⁻⁴

Iron-sulfur [Fe-S] clusters are ubiquitous and evolutionary prosthetic groups that are required to sustain fundamental life processes.⁵ Three different types of [Fe-S] cluster biosynthetic systems (Nif (nitrogen fixation specific), Isc (iron sulfur cluster), and Suf (sulfur utilization factor)) have been discovered/proposed. Importantly, the biosynthesis of [Fe-S] clusters, constructed by the requirement of cysteine desulfurase and the participation of an [Fe-S] cluster scaffold protein, includes the following steps: (i) mobilizing iron and sulfur atoms from their storage sources in nontoxic forms, (ii) assembling them into an [Fe-S] core, and (iii) insertion of the assembled [Fe-S] core into apoprotein.⁶ However, design and interpretation of such in vitro "cluster transfer" experiments are difficult because some apo-

- (1) (a) Palmer, R. M. J.; Ferrige, A. G.; Moncada, S. *Nature* **1987**, *327*, 524–526. (b) Ignarro, L. J.; Buga, G. M.; Wood, K. S.; Byrns, R. E.; Chaudhuri, G. *Proc. Natl. Acad. Sci. U.S.A.* **1987**, *84*, 9265–9269. (c) Furchgott, R. F. *Angew. Chem., Int. Ed.* **1999**, *38*, 1870–1880. (d) Alderton, W. K.; Cooper, C. E.; Knowles, R. G. *Biochem. J.* **2001**, *357*, 593–615.
- (2) (a) Butler, A. R.; Megson, I. L. *Chem. Rev.* **2002**, *102*, 1155–1166. (b) Szaciłowski, K.; Chmura, A.; Stasička, Z. *Coord. Chem. Rev.* **2005**, *249*, 2408–2436. (c) De Groote, M. A.; Fang, F. C. *Clin. Infect. Dis.* **1995**, *21*, s162–s165. (d) Nathan, C. F.; Hibbs, J. B., Jr. *Curr. Opin. Immunol.* **1991**, *3*, 65–70. (e) Lorsbach, R. B.; Murphy, W. J.; Lowenstein, C. J.; Snyder, S. H.; Russell, S. W. *J. Biol. Chem.* **1993**, *268*, 1908–1913. (f) Moncada, S.; Higgs, A. *N. Engl. J. Med.* **1993**, *329*, 2002–2012.
- (3) Ueno, T.; Susuki, Y.; Fujii, S.; Vanin, A. F.; Yoshimura, T. *Biochem. Pharmacol.* **2002**, *63*, 485–493.

- (4) (a) Foster, M. W.; Cowan, J. A. *J. Am. Chem. Soc.* **1999**, *121*, 4093–4100. (b) Cooper, C. E. *Biochim. Biophys. Acta* **1999**, *1411*, 290–309.

- (5) (a) Calzolari, L.; Zhou, Z.-H.; Adams, M. W. W.; Lamar, G. N. *J. Am. Chem. Soc.* **1996**, *118*, 2513–2514. (b) Flint, D. H.; Allen, R. M. *Chem. Rev.* **1996**, *96*, 2315–2334. (c) Beinert, H.; Kennedy, M. C.; Stout, C. D. *Chem. Rev.* **1996**, *96*, 2335–2373. (d) Dobbek, H.; Svetlitchnyi, V.; Gremer, L.; Huber, R.; Meyer, O. *Science* **2001**, *293*, 1281–1285. (e) Hedderich, R.; Albracht, S. P.; Linder, D.; Koch, J.; Thauer, R. K. *FEBS Lett.* **1992**, *298*, 65–68. (f) Wu, C. K.; Dailey, H. A.; Rose, J. P.; Burden, A.; Sellers, V. M.; Wang, B. C. *Nat. Struct. Biol.* **2001**, *8*, 156–160. (g) Berkovitch, F.; Nicolet, Y.; Wan, J. T.; Jarrett, J. T.; Drennan, C. L. *Science* **2004**, *303*, 76–79.

[Fe-S] proteins can be spontaneously activated by the simple addition of Fe^{2+} and SH^-/S .⁷ A rational mechanism is that the [Fe-S] core is delivered to apo-[Fe-S] protein by specific carrier proteins.⁷

NO has been demonstrated to react with the [Fe-S] clusters of several proteins including succinate dehydrogenase, nitrogenase, succinate-Q reductase, mitochondrial aconitase, cytosolic aconitase, HiPIP, endonuclease III, mammalian ferrochelatase, and SoxR to form the monomeric, EPR-active DNICs.^{5a,8-14} Recently, Ding and co-workers showed that when *Escherichia coli* (*E. coli*) cells are exposed to nitric oxide, the ferredoxin [2Fe-2S] clusters are modified to form protein-bound dinitrosyl iron complexes. In the repair of NO-modified ferredoxin [2Fe-2S] clusters, the dinitrosyl iron complexes can be directly transformed back to the ferredoxin [2Fe-2S] cluster by cysteine desulfurase (IscS) and L-cysteine in vitro with no need of the addition of iron or any other protein components.^{14a,b} Removal of the dinitrosyl iron complex from ferredoxin preventing reassembly of the [2Fe-2S] cluster suggests the iron in the dinitrosyl iron complex may be recycled for the reassembly of an iron-sulfur cluster in the protein.^{14a,b} Drapier and co-workers demonstrated that nitric oxide converts IRP-1 (iron regulatory proteins) from a [4Fe-4S] aconitase to a trans-regulatory protein through [Fe-S] cluster disassembly. Reversibly, NO-modified aconitases repairing of the [4Fe-4S] clusters was also observed.^{14c} In addition, the [4Fe-4S] cluster of the *E. coli* endonuclease III modified by NO forming the protein-bound dinitrosyl iron complex in vitro/in vivo and the NO-modified [4Fe-4S] cluster being efficiently repaired in aerobically growing *E. coli* cells were also reported.¹²

In chemistry, synthetic routes to the [2Fe-2S] clusters $[(\text{SR})_2\text{Fe}(\mu\text{-S})_2\text{Fe}(\text{SR})_2]^{2-}$ (R = alkyl, aryl) were discovered shortly after the preparation of the first [4Fe-4S] cluster, and the isolation/characterization of mononuclear rubredoxin $[\text{Fe}(\text{SR})_4]^{2-/1-}$ subsequently followed.¹⁵ Recently, the formation pathway of the anionic $\{\text{Fe}(\text{NO})_2\}$ DNICs $[(\text{NO})_2\text{Fe}(\text{SR})_2]^-$ from nitrosylation of the biomimetic oxidized and reduced form of rubredoxin $[\text{Fe}(\text{SR})_4]^{2-/1-}$ (R = Ph, Et) and the reactivity of the mononitrosyl tris(thiolate) complexes $[(\text{NO})\text{Fe}(\text{SR})_3]^-$, an intermediate for the conversion of $[\text{Fe}(\text{SR})_4]^{2-/1-}$ into DNICs

in the presence of $\text{NO}_{(g)}$, were elucidated.^{16,17} In addition, we also demonstrated that nitrosylation of the [2Fe-2S] cluster $[\text{S}_5\text{Fe}(\mu\text{-S})_2\text{FeS}_5]^{2-}$ yielding $[(\text{NO})_2\text{FeS}_5]^-$ and the reversible transformation of complex $[(\text{NO})_2\text{FeS}_5]^-$ to the $[\text{S}_3\text{Fe}(\mu\text{-S})_2\text{FeS}_5]^{2-}$ by photolysis in the presence of the NO-acceptor reagent $[(\text{C}_4\text{H}_8\text{O})\text{Fe}(\text{S},\text{S}-\text{C}_6\text{H}_4)_2]^-$ are consistent with reports of the in vitro degradation of ferredoxin [2Fe-2S] clusters to DNICs and the repair of NO-modified [2Fe-2S] ferredoxin by cysteine desulfurase and L-cysteine.¹⁸ In this report, an exciting advance in this topic, the transformation of DNICs into [4Fe-4S] clusters $[\text{Fe}_4\text{S}_4(\text{SR})_4]^{2-}$ in the presence of the reduced/oxidized-form $[\text{Fe}(\text{SPh})_4]^{2-/1-}$ and sulfur-donor species, was demonstrated.

Results and Discussion

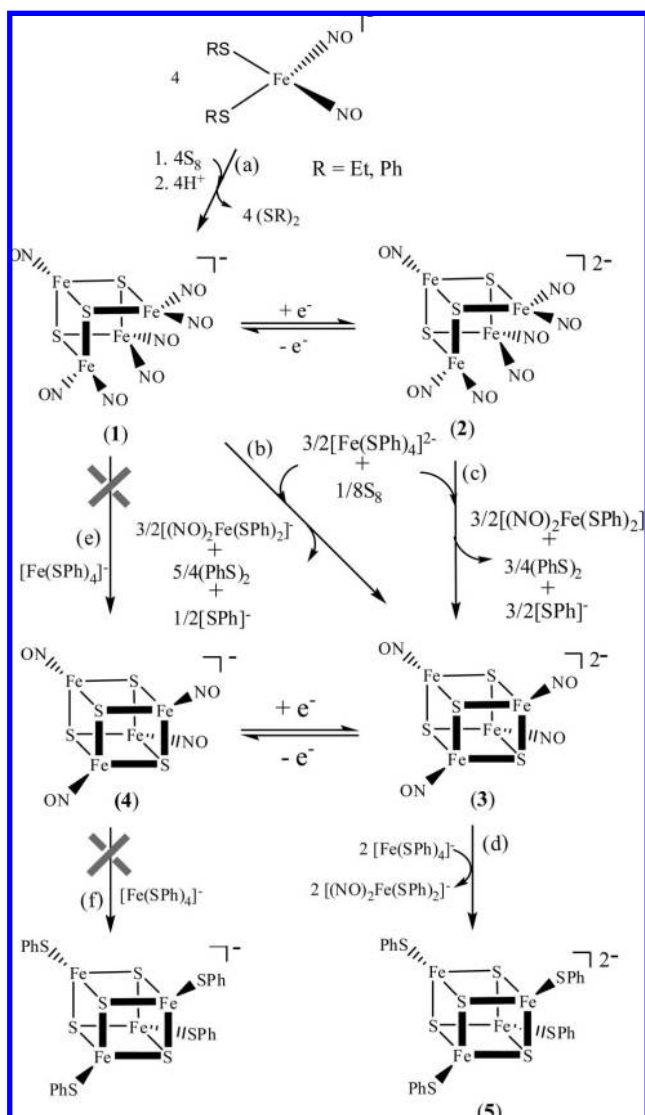
Transformation of $[(\text{NO})_2\text{Fe}(\text{SR})_2]^-$ (R = Et, Ph) into $[\text{Fe}_4\text{S}_3(\text{NO})_7]^-$ (1). Consistent with the facile conversion of DNICs $[(\text{NO})_2\text{Fe}(\text{SR})_2]^-$ into Roussin's black salt (RBS) $[\text{Fe}_4\text{S}_3(\text{NO})_7]^-$ (1) in the presence of S_8 via the intermediate $[(\text{NO})_2\text{FeS}_5]^-$ observed in the previous study,¹⁸⁻²⁰ quantitative transformation of DNICs $[(\text{NO})_2\text{Fe}(\text{SET})_2]^-$ to complex **1** was displayed and monitored by IR ν_{NO} spectra. The shift of the NO stretching frequency from 1715 s, 1673 s cm^{-1} to 1790 w, 1740 s, 1707 m cm^{-1} is consistent with the formation of complex $[\text{Na}-18\text{-crown-6-ether}][\text{Fe}_4\text{S}_3(\text{NO})_7]^-$ (1) when a THF solution of $[(\text{NO})_2\text{Fe}(\text{SET})_2]^-$ was reacted with S_8 in a 1:1 molar ratio, followed by the addition of HBF_4 into the mixture solution (Scheme 1a).¹⁸⁻²⁰

Conversion of Complex $[\text{Fe}_4\text{S}_3(\text{NO})_7]^{2-}$ (2) into $[\text{Fe}_4\text{S}_4(\text{NO})_4]^{2-}$ (3). The conversion of complex $[\text{Fe}_4\text{S}_3(\text{NO})_7]^{2-}$ (2),²¹ obtained from reduction of complex **1** by $[\text{Na}][\text{biphenyl}]$, into complex $[\text{Fe}_4\text{S}_4(\text{NO})_4]^{2-}$ (3), characterized by IR, UV-vis, and single-crystal X-ray diffraction, was carried out when complex **2** was treated with 1.5 equiv of $[\text{Fe}(\text{SPh})_4]^{2-}$ and the subsequent addition of 1/8 equiv of S_8 in CH_3CN at ambient temperature (Scheme 1b).²² Quantitative conversion of complex **2** to complex **3** and $[(\text{NO})_2\text{Fe}(\text{SPh})_2]^-$ in the presence of $[\text{Fe}(\text{SPh})_4]^{2-}$ and S_8 was monitored by IR. The shift of IR ν_{NO} stretching frequencies from 1748 m, 1690 s, 1660 sh cm^{-1} to 1743 s, 1708 s, 1697 sh cm^{-1} implicated the formation of the known $[(\text{NO})_2\text{Fe}(\text{SPh})_2]^-$ accompanied by the proposed intermediate $[\text{Fe}_4\text{S}_3(\text{SPh})(\text{NO})_4]^{2-}$ (A) when complex **2** was reacted with 1.5 equiv of $[\text{Fe}(\text{SPh})_4]^{2-}$ in CH_3CN at room temperature

- (6) (a) Rouault, T. A.; Tong, W.-H. *Nat. Rev. Mol. Cell Biol.* **2005**, *6*, 345-351. (b) Balk, J.; Lill, R. *ChemBioChem* **2004**, *5*, 1044-1049. (c) Gerber, J.; Lill, R. *Mitochondrion* **2002**, *2*, 71-86. (d) Fontecave, M.; Ollagnier-de Choudens, S. *Arch. Biochem. Biophys.* **2008**, *474*, 226-237.
- (7) Lill, R.; Muhlenhoff, U. *Trends Biochem. Sci.* **2005**, *30*, 133-141.
- (8) Kennedy, M. C.; Antholine, W. E.; Beinert, H. *J. Biol. Chem.* **1997**, *272*, 20340-20347.
- (9) Salerno, J. C.; Ohnishi, T.; Lim, J.; King, T. E. *Biochem. Biophys. Res. Commun.* **1976**, *73*, 833-840.
- (10) Meyer, J. *Arch. Biochem. Biophys.* **1981**, *210*, 246-256.
- (11) Welter, R.; Yu, L.; Yu, C.-A. *Arch. Biochem. Biophys.* **1996**, *331*, 9-14.
- (12) Rogers, P. A.; Eide, L.; Klungland, A.; Ding, H. *DNA Repair* **2003**, *2*, 809-817.
- (13) Sellers, V. M.; Johnson, M. K.; Dailey, H. A. *Biochemistry* **1996**, *35*, 2699-2704.
- (14) (a) Ding, H.; Demple, B. *Proc. Natl. Acad. Sci. U.S.A.* **2000**, *97*, 5146-5150. (b) Yang, W.; Rogers, P. A.; Ding, H. *J. Biol. Chem.* **2002**, *277*, 12868-12873. (c) Bouton, C.; Chauveau, M.-J.; Lazereg, S.; Drapier, J.-C. *J. Biol. Chem.* **2002**, *277*, 31220-31227.
- (15) (a) Rao, P. V.; Holm, R. H. *Chem. Rev.* **2004**, *104*, 527-559. (b) Mayerle, J. J.; Denmark, S. E.; DePamphilis, B. V.; Ibers, J. A.; Holm, R. H. *J. Am. Chem. Soc.* **1975**, *97*, 1032-1045. (c) Hagen, K. S.; Watson, A. D.; Holm, R. H. *J. Am. Chem. Soc.* **1983**, *105*, 3905-3913. (d) Maelia, L. E.; Millar, M.; Koch, S. A. *Inorg. Chem.* **1992**, *31*, 4594-4600. (e) Chang, S.; Koch, S. A. *J. Inorg. Biochem.* **2007**, *101*, 1758-1759.

- (16) Harrop, T. C.; Song, D. T.; Lippard, S. J. *J. Am. Chem. Soc.* **2006**, *128*, 3528-3529.
- (17) Lu, T.-T.; Chiou, S.-J.; Chen, C.-Y.; Liaw, W.-F. *Inorg. Chem.* **2006**, *45*, 8799-8806.
- (18) Tsai, M.-L.; Chen, C.-C.; Hsu, I.-J.; Ke, S.-C.; Hsieh, C.-H.; Chiang, K.-A.; Lee, G.-H.; Wang, Y.; Liaw, W.-F. *Inorg. Chem.* **2004**, *43*, 5159-5167.
- (19) (a) Chen, T.-N.; Lo, F.-C.; Tsai, M.-L.; Shih, K.-N.; Chiang, M.-H.; Lee, G.-H.; Liaw, W.-F. *Inorg. Chim. Acta* **2006**, *359*, 2525-2533. (b) Butler, A. R.; Glidewell, C.; Hyde, A. R.; Walton, J. C. *Polyhedron* **1985**, *4*, 797-809.
- (20) (a) Tsai, F.-T.; Chiou, S.-J.; Tsai, M.-C.; Tsai, M.-L.; Huang, H.-W.; Chiang, M.-H.; Liaw, W.-F. *Inorg. Chem.* **2005**, *44*, 5872-5881. (b) Hung, M.-C.; Tsai, M.-C.; Lee, G.-H.; Liaw, W.-F. *Inorg. Chem.* **2006**, *45*, 6041-6047. (c) Tsai, M.-L.; Liaw, W.-F. *Inorg. Chem.* **2006**, *45*, 6583-6585. (d) Tsou, C.-C.; Lu, T.-T.; Liaw, W.-F. *J. Am. Chem. Soc.* **2007**, *129*, 12626-12627. (e) Lu, T.-T.; Tsou, C.-C.; Huang, H.-W.; Hsu, I.-J.; Chen, J.-M.; Kuo, T.-S.; Wang, Y.; Liaw, W.-F. *Inorg. Chem.* **2008**, *47*, 6040-6050. (f) Huang, H.-W.; Tsou, C.-C.; Kuo, T.-S.; Liaw, W.-F. *Inorg. Chem.* **2008**, *47*, 2196-2204.
- (21) D'Addario, S.; Demartin, F.; Grossi, L.; Iapalucci, M. C.; Laschi, F.; Longoni, G.; Zanello, P. *Inorg. Chem.* **1993**, *32*, 1153-1160.
- (22) (a) Chu, C. T. W.; Lo, F. Y. K.; Dahl, L. F. *J. Am. Chem. Soc.* **1982**, *104*, 3409-3422. (b) Kalyvas, H.; Coucouvanis, D. *Inorg. Chem.* **2006**, *45*, 8462-8464.

Scheme 1



for 3 h, and thereafter, the appearance of ν_{NO} stretching frequencies (1743 s, 1697 s, 1660 s cm^{-1}) confirmed the formation of complex **3** and $[(\text{NO})_2\text{Fe}(\text{SPh})_2]^-$ upon subsequent addition of 1/8 equiv of S_8 into the mixture solution and stirring at room temperature overnight. The conversion of complex **2** into complex **3** in the presence of $[\text{Fe}(\text{SPh})_4]^{2-}$ and S_8 may be accounted for by the following reaction sequence, as shown in Scheme 2a,b: nitrosylation of $[\text{Fe}(\text{SPh})_4]^{2-}$ by complex **2** leads to $[(\text{NO})_2\text{Fe}(\text{SPh})_2]^-$ along with $[\text{SPh}]^-$ ^{16,17} and the buildup of the proposed intermediate **A**. The subsequent reductive elimination of diphenyl disulfide of intermediate **A** accompanied by the concurrent oxidative addition of S atom yields complex **3** (Scheme 2b). This rationalizes the absence of mononitrosyl iron complex $[(\text{NO})\text{Fe}(\text{SPh})_3]^-$ observed spectrally in this transformation process.^{16,17} It is presumed that the rapid intermolecular addition of a generated thiyl radical to the adjacent $[\text{Fe}_4\text{S}_3(\text{NO})_4]^{2-}$ core occurred to yield intermediate **A** (Scheme 2a), since two NO radicals binding to an electron-rich iron(II) center of complex $[\text{Fe}(\text{SPh})_4]^{2-}$, triggering displacement of thiolates ($[\text{SPh}]^-$), and the subsequent reductive elimination of thiyl radical, yielding diphenyl disulfide, are known.¹⁷ Presumably, this highly reactive intermediate **A**, generated in the course of NO-radical transfer from complex **2** to $[\text{Fe}(\text{SPh})_4]^{2-}$, retains

Scheme 2

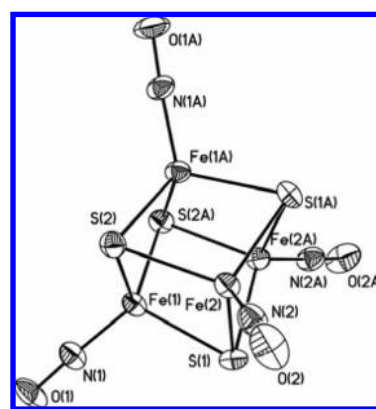
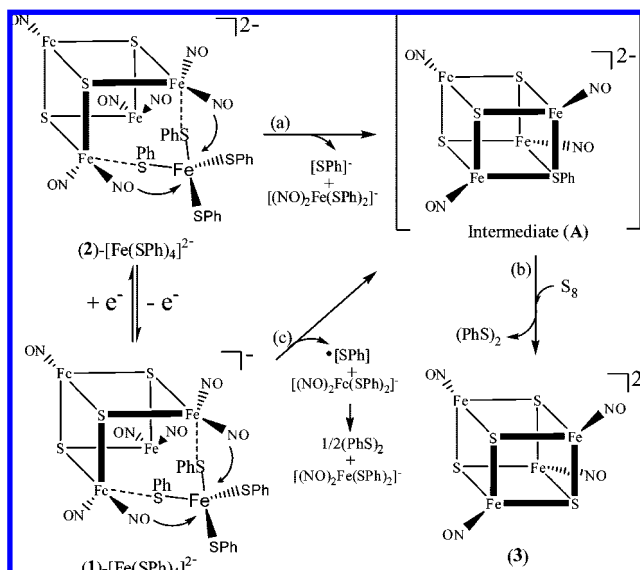


Figure 1. ORTEP drawing and labeling scheme of the $[\text{Fe}_4\text{S}_4(\text{NO})_4]^{2-}$ unit in the $[\text{Me}_4\text{N}]^+$ salt with thermal ellipsoids drawn at 50% probability. Selected bond distances (\AA) and angles (deg): $\text{Fe}(1)\cdots\text{Fe}(2)$ 2.6681(15); $\text{Fe}(1)\cdots\text{Fe}(1\text{A})$ 2.795(2); $\text{Fe}(1)\cdots\text{Fe}(2\text{A})$ 2.7147(15); $\text{Fe}(2)\cdots\text{Fe}(1\text{A})$ 2.7147(15); $\text{Fe}(2)\cdots\text{Fe}(2\text{A})$ 2.771(2); $\text{Fe}(1)-\text{S}(1)$ 2.228(2); $\text{Fe}(1)-\text{S}(2)$ 2.250(2); $\text{Fe}(1)-\text{S}(2\text{A})$ 2.253(2); $\text{Fe}(2)-\text{S}(2)$ 2.234(2); $\text{Fe}(2)-\text{S}(1)$ 2.239(2); $\text{Fe}(2)-\text{S}(1\text{A})$ 2.255(2); $\text{S}(1)-\text{Fe}(2\text{A})$ 2.255(2); $\text{S}(2)-\text{Fe}(1\text{A})$ 2.253(2); $\text{Fe}(1)-\text{N}(1)$ 1.666(7); $\text{Fe}(2)-\text{N}(2)$ 1.665(7); $\text{O}(1)-\text{N}(1)$ 1.180(8); $\text{O}(2)-\text{N}(2)$ 1.193(8); $\text{S}(1)-\text{Fe}(1)-\text{S}(2)$ 105.72(8); $\text{S}(1)-\text{S}(1)-\text{S}(2)$ 103.93(8); $\text{S}(2)-\text{Fe}(1)-\text{S}(2\text{A})$ 100.07(8); $\text{S}(2)-\text{Fe}(2)-\text{S}(1)$ 105.86(9); $\text{S}(2)-\text{Fe}(2)-\text{S}(1\text{A})$ 103.66(8); $\text{S}(1)-\text{Fe}(2)-\text{S}(1\text{A})$ 100.77(8); $\text{Fe}(1)-\text{S}(1)-\text{Fe}(2)$ 73.35(7); $\text{Fe}(1)-\text{S}(1)-\text{Fe}(2\text{A})$ 74.55(7); $\text{Fe}(2)-\text{S}(1)-\text{Fe}(2\text{A})$ 76.12(7); $\text{Fe}(2)-\text{S}(2)-\text{Fe}(1)$ 73.01(7); $\text{Fe}(2)-\text{S}(2)-\text{Fe}(1\text{A})$ 74.45(7); $\text{Fe}(1)-\text{S}(2)-\text{Fe}(1\text{A})$ 76.74(7); $\text{O}(1)-\text{N}(1)-\text{Fe}(1)$ 176.5(6); $\text{O}(2)-\text{N}(2)-\text{Fe}(2)$ 176.7(7).

the cubane-like geometry and triggers the insertion/oxidative addition of S to yield complex **3**.

Single-Crystal X-ray Structure of Complex $[\text{Me}_4\text{N}][\text{Fe}_4\text{S}_4(\text{NO})_4]^{2-}$ (3-Me₄N**).** Compared to the known complex **4**, displaying an IR ν_{NO} stretching frequency at 1729 cm^{-1} (CH_3CN),^{22a} complex **3-Me₄N** exhibits a diagnostic IR ν_{NO} stretching frequency at 1660 cm^{-1} (CH_3CN). Presumably, complex **3-Me₄N**, containing $\{\text{Fe}(\text{NO})\}^8\text{-}\{\text{Fe}(\text{NO})\}^8\{\text{Fe}(\text{NO})\}^7\text{-}\{\text{Fe}(\text{NO})\}^7$ coupling, may rationalize the absence of paramagnetism and the EPR signal. An ORTEP diagram of $[\text{Fe}_4\text{S}_4(\text{NO})_4]^{2-}$ unit in the $[\text{Me}_4\text{N}]^+$ salt is depicted in Figure 1, and selected bond dimensions are presented in the figure caption. As shown in Table 1, the apparently longer $\text{Fe}\cdots\text{Fe}$ distance (average 2.722(2) \AA) of complex **3-Me₄N**, compared

Table 1. Selected Metric Data for $[\text{Fe}_4\text{S}_4(\text{NO})_4]^{0/1-2-a 22}$

	$[\text{Fe}_4\text{S}_4(\text{NO})_4]$	$[\text{Fe}_4\text{S}_4(\text{NO})_4]^{2-}$ ^b	$[\text{Fe}_4\text{S}_4(\text{NO})_4]^{2-}$ ^c
Fe···Fe (Å)	2.651(1)	2.693(1)	2.722(2)
Fe–S (Å)	2.217(2)	2.231(2)	2.243(2)
Fe–N (Å)	1.663(6)	1.659(5)	1.666(7)
N–O (Å)	1.155(7)	1.168(6)	1.187(8)
S···S (Å)	3.503	3.510	3.512
Fe–S–Fe (deg)	73.43(6)	74.25(6)	74.70(7)
S–Fe–S (deg)	104.37(7)	103.76(7)	103.34(9)
Fe–N–O (deg)	177.6(5)	177.5(6)	176.6(7)

^a Average bond distances and angles. ^b $[\text{K}(2,2,2\text{-crypt})]^+$ salt. ^c $[\text{Me}_4\text{N}]^+$ salt.

to those of 2.651(1) and 2.693(1) Å in complex $[\text{Fe}_4\text{S}_4(\text{NO})_4]$ and complex **4**,²² respectively, indicates the weaker Fe···Fe interaction in complex **3-Me₄N**. Presumably, the electronic perturbation caused by the reduction of complex **4** reduces the Fe···Fe interaction to relieve the richness of electron density surrounding the delocalized $[\{\text{Fe}(\text{NO})\}^8\text{-}\{\text{Fe}(\text{NO})\}^7][\text{Fe}_4(\mu\text{-S})_4]$ core. Compared to the average Fe–S bond distances of 2.217(2) and 2.231(2) Å, respectively, found in complex $[\text{Fe}_4\text{S}_4(\text{NO})_4]$ and complex **4**,²² the longer Fe–S distances of 2.243(2) Å (average) observed in complex **3-Me₄N** indicate that reduction of complex **4** yielding **3-Me₄N** results in the elongation of the Fe–S distances.

Conversion of Complex 1 into $[\text{Fe}_4\text{S}_4(\text{NO})_4]^{2-}$ (3**).** In contrast to the inertness of complex **1** toward the oxidized-form $[\text{Fe}(\text{SPh})_4]^-$ (Scheme 1e), addition of 1.5 equiv of $[\text{Fe}(\text{SPh})_4]^{2-}$ to a CH_3CN solution of complex **1** ($E_{1/2} = -0.50$ V vs SCE for $[\text{Fe}(\text{SPh})_4]^{2-/1-}$; $E_{1/2} = -0.68$ V vs SCE for $[\text{Fe}_4\text{S}_3(\text{NO})_7]^{2-/1-}$),^{15d,21} and the subsequent addition of 1/8 equiv of S_8 powder into the mixture solution yielded the cubane cluster $[\text{Fe}_4\text{S}_4(\text{NO})_4]^{2-}$ (**3**) and $[(\text{NO})_2\text{Fe}(\text{SPh})_2]^-$, characterized by IR, when the mixture solution was stirred at ambient temperature for 36 h (Scheme 1b).^{20,22} The IR ν_{NO} stretching frequencies 1743, 1697, 1660 cm^{-1} , shifting from 1800, 1747, 1707 cm^{-1} , via the appearance of IR ν_{NO} 1743 s, 1708 s, 1697 sh cm^{-1} , are in accordance with the formation of $[(\text{NO})_2\text{Fe}(\text{SPh})_2]^-$ and complex **3**. This result suggests that the electron-deficient $[\text{Fe}_4\text{S}_3(\text{NO})_4]^-$ core, resulting from trans-nitrosylation of $[\text{Fe}(\text{SPh})_4]^{2-}$ by complex **1**, prefers the coordination of the released $[\text{SPh}]^-$ from trans-nitrosylation between $[\text{Fe}(\text{SPh})_4]^{2-}$ and complex **1** to yield intermediate **A** (as shown in Scheme 2c), in contrast to the coordination of $[\text{SPh}]^-$ to the $[\text{Fe}_4\text{S}_3(\text{NO})_4]^{2-}$ core, yielding intermediate **A**, observed in the reaction of complex **2** and $[\text{Fe}(\text{SPh})_4]^{2-}$. Thus, the absence of the released $[\text{SPh}]^-$ from reaction of $[\text{Fe}(\text{SPh})_4]^-$ and complex **1** coordinated to the electron-deficient $[\text{Fe}_4\text{S}_3(\text{NO})_4]^-$ core yielding intermediate **A** may explain the observed inertness of complex **1** toward the oxidized-form $[\text{Fe}(\text{SPh})_4]^-$. That is, the $[\text{SPh}]^-$ -coordinated ligand may promote the stability of the electron-deficient $[\text{Fe}_4\text{S}_3(\text{NO})_4]^-$ core, in contrast to the thiyl radical $[\text{SPh}]^\cdot$ coordinated to the $[\text{Fe}_4\text{S}_3(\text{NO})_4]^{2-}$ core, yielding intermediate **A**.

Alternatively, addition of 1 equiv of the oxidized-form $[\text{Fe}(\text{SPh})_4]^-$ into a CH_3CN solution of complex **2** and the subsequent addition of 1/8 equiv of S_8 powder into the mixture solution also led to the formation of complex **3**, $[(\text{NO})_2\text{Fe}(\text{SPh})_2]^-$, and the remaining complex **1**, characterized by IR and UV–vis, when the mixture solution was stirred at ambient temperature for 36 h. Presumably, complex **3** was produced upon the initial reduction of complex $[\text{Fe}(\text{SPh})_4]^-$ by complex **2**, yielding $[\text{Fe}(\text{SPh})_4]^{2-}$ and complex **1**, the subsequent nitrosylation of $[\text{Fe}(\text{SPh})_4]^{2-}$ by complex **1**, yielding $[(\text{NO})_2\text{Fe}(\text{SPh})_2]^-$ and intermediate **A**, followed by the sequen-

tial reductive elimination of diphenyl disulfide of intermediate **A** and the concomitant oxidative addition of S, as observed in the reaction of complex **2** and $[\text{Fe}(\text{SPh})_4]^{2-}$.

These results implicate that complexes **2/1** optimize the electronic property of the $[\text{Fe}_4\text{S}_3(\text{NO})_7]^{2-/1-}$ core to serve as a good NO-donor species, and the highly reactive intermediate **A** optimizes the electronic property of $[\text{Fe}_4\text{S}_3(\text{SPh})(\text{NO})_4]^{2-}$ core for its required S insertion/oxidative addition function.

Conversion of Complex 3 into $[\text{Fe}_4\text{S}_4(\text{SPh})_4]^{2-}$ (5**).** To follow up on our earlier study with a more complete understanding of the conversion of DNICs into $[\text{2Fe-2S}]$ clusters and their relevance as a model of the transformation of NO-modified ferredoxin $[\text{2Fe-2S}]$ and $[\text{4Fe-4S}]$ clusters,¹⁸ the reactivity of complex **3** toward $[\text{Fe}(\text{SPh})_4]^-$ was investigated. In contrast to the inertness of complex **4** toward the biomimetic oxidized-form rubredoxin $[\text{Fe}(\text{SPh})_4]^-$ (Scheme 1f), the direct transformation of complex **3** to the known complex $[\text{Fe}_4\text{S}_4(\text{SPh})_4]^{2-}$ (**5**) accompanied by the formation of byproduct $[(\text{NO})_2\text{Fe}(\text{SPh})_2]^-$ was displayed when a CH_3CN solution of complex **3** was treated with $[\text{Fe}(\text{SPh})_4]^-$ in a 1:2 molar ratio for 10 min at ambient temperature (Scheme 1d). The conversion of complex **3** to **5** was monitored and characterized by IR, ¹H NMR, and UV–vis spectrometry; the formation of one absorption band at 447 nm and the shift of the ν_{NO} stretching frequencies from 1660 cm^{-1} to 1743 s, 1697 cm^{-1} confirmed the formation of complex **5** and $[(\text{NO})_2\text{Fe}(\text{SPh})_2]^-$.^{15,20} Complex **5** was isolated in 45% yield after the solution mixture was separated from $[(\text{NO})_2\text{Fe}(\text{SPh})_2]^-$ and identified by ¹H NMR.¹⁵ The transformation of complex **3** into complex **5** in the presence of $[\text{Fe}(\text{SPh})_4]^-$ may be accounted for by the following reaction sequences: the process for the rapid conversion of complex **3** into complex **5** along with $[(\text{NO})_2\text{Fe}(\text{SPh})_2]^-$ is a mechanism of NO radical–thiyl radical ($[\text{PhS}]^\cdot$) exchange reaction. NO scavenging by the NO-acceptor of the biomimetic oxidized-form rubredoxin $[\text{Fe}(\text{SPh})_4]^-$, triggering the reductive elimination of the coordinated phenylthiolate of $[\text{Fe}(\text{SPh})_4]^-$ to generate thiyl radical ($[\text{PhS}]^\cdot$), with concurrent binding to the $[\text{Fe}_4\text{S}_4]^{2-}$ core, rationalizes the simultaneous formation of complex **5** and $[(\text{NO})_2\text{Fe}(\text{SPh})_2]^-$ (Scheme 1d). Thus, the presence of biomimetic oxidized-form rubredoxin $[\text{Fe}(\text{SPh})_4]^-$ appears to be crucial in triggering the conversion of complex **3** to complex **5** ($E_{1/2} = -0.50$ V vs SCE for $[\text{Fe}(\text{SPh})_4]^{2-/1-}$ and $E_{1/2} = -0.65$ V vs SCE for $[\text{Fe}_4\text{S}_4(\text{NO})_4]^{2-/1-}$).^{15d,22a}

Conclusion and Comments

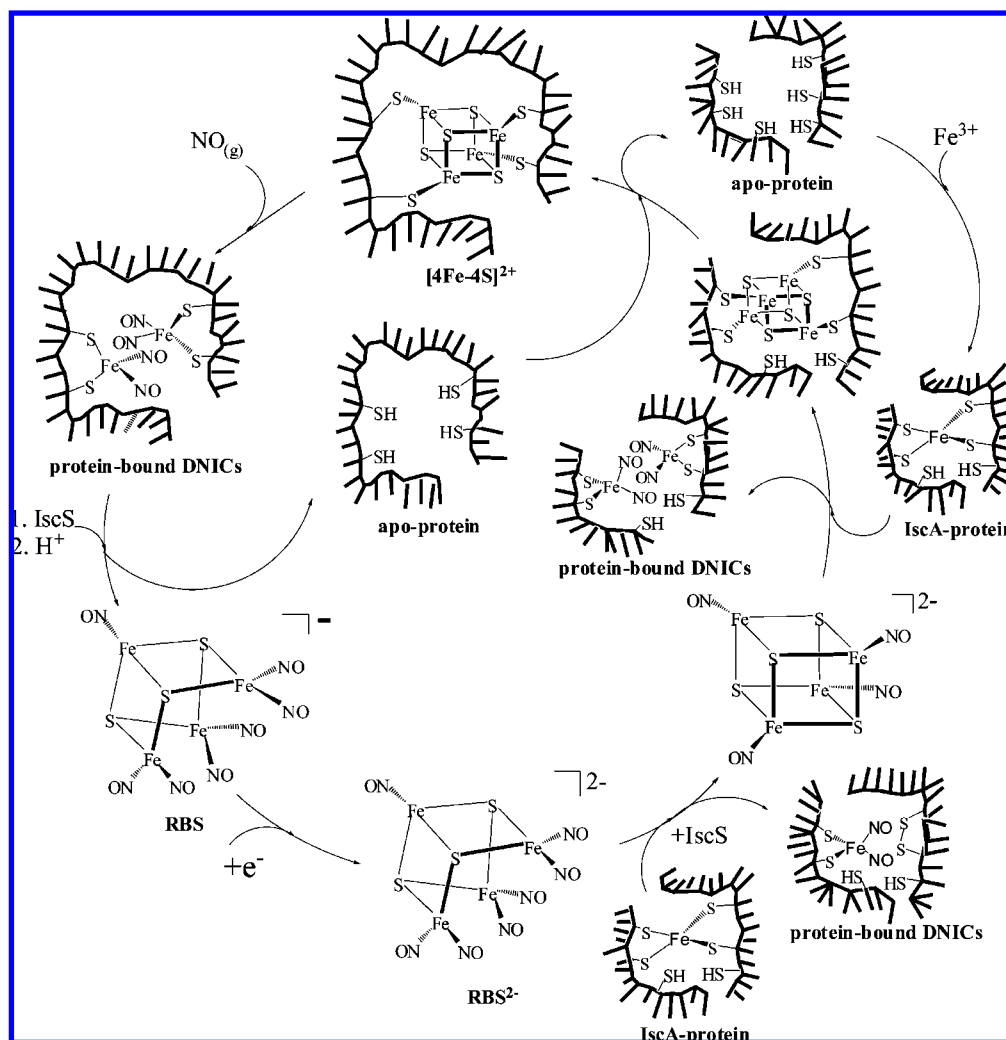
Studies on the transformation of dinitrosyl iron complexes $[(\text{NO})_2\text{Fe}(\text{SR})_2]^-$ back to the known $[\text{4Fe-4S}]$ cluster **5** have led to the following results.

(1) This study demonstrates that DNICs $[(\text{NO})_2\text{Fe}(\text{SR})_2]^-$ can be converted back to $[\text{4Fe-4S}]$ cluster **5** in the presence of $[\text{Fe}(\text{SPh})_4]^{2-/1-}$ and S-donor species S_8 via a reassembling process ($[(\text{RS})_2\text{Fe}(\text{NO})_2]^- \rightarrow [\text{Fe}_4\text{S}_3(\text{NO})_7]^-$ (**1**)/ $[\text{Fe}_4\text{S}_3(\text{NO})_7]^{2-}$ (**2**) $\rightarrow [\text{Fe}_4\text{S}_4(\text{NO})_4]^{2-}$ (**3**) $\rightarrow [\text{Fe}_4\text{S}_4(\text{SPh})_4]^{2-}$ (**5**)).

(2) In contrast to complexes **1** and **2** serving as NO-radical-donor species toward $[\text{Fe}(\text{SPh})_4]^{2-}$, the proposed degradation species $[\text{Fe}_4\text{S}_3(\text{NO})_4]^{2-}$ and $[\text{Fe}_4\text{S}_3(\text{NO})_4]^-$ derived from NO release of complexes **2** and **1** act as a thiyl-radical acceptor and phenylthiolate acceptor, respectively, to yield the proposed $[\text{Fe}_4\text{S}_3(\text{SPh})(\text{NO})_4]^{2-}$ (**A**) intermediate.

(3) The electronic richness of the proposed intermediate $[\text{Fe}_4\text{S}_3(\text{SPh})(\text{NO})_4]^{2-}$ (**A**), derived from trans-nitrosylation between **2** and $[\text{Fe}(\text{SPh})_4]^{2-}$ or trans-nitrosylation between complex **1** and $[\text{Fe}(\text{SPh})_4]^{2-}$, triggers reductive elimination of $(\text{PhS})_2$

Scheme 3



accompanied by the concurrent oxidative addition of S atom to yield complex **3**.

(4) The effective NO-accepting functionality of the biomimetic oxidized-form rubredoxin $[\text{Fe}(\text{SPh})_4]^-$ is responsible for the NO radical–thiyl radical exchange reaction in the transformation of complex **3** to complex **5**. These results illustrate that complex **2** acts as a pure NO-donor species, whereas complex **3** prefers NO radical–thiyl radical exchange reaction to yield complex **5**.

It has been known that repair of DNICs derived from nitrosylation of a $[\text{4Fe-4S}]$ cluster of endonuclease III back to $[\text{4Fe-4S}]$ was achieved by addition of ferrous ion, cysteine, and IscS.¹² Also, *in vitro* repair of DNICs to $[\text{2Fe-2S}]$ protein directed by IscS as well as L-cysteine and *in vivo* $[\text{2Fe-2S}]$ protein construction from assembly of cysteine, sulfur derived from IscS, and free iron released from DNICs were proposed.^{14b} The biomimetic study of the degradation of $[\text{Fe-S}]$ clusters and repair of NO-modified $[\text{Fe-S}]$ clusters (DNICs) that lead to initial insights concerning the formation mechanism of $[\text{Fe-S}]$ clusters may lead to an understanding of the fundamental features of $[\text{Fe-S}]$ cluster biogenesis. This study may decipher that the mechanism for the $[\text{4Fe-4S}]$ iron–sulfur protein biosynthesis is as follows: a preassembled $[\text{Fe}_4\text{S}_4(\text{NO})_4]^{2-}$ cluster derived from the conversion of protein-bound DNICs is transferred from solution to a site in a protein by exchanging its simple NO

ligands for cysteinate groups of rubredoxin (Scheme 3). That is, protein-bound DNICs derived from nitrosative stress-damaged $[\text{4Fe-4S}]$ iron sulfur clusters can be converted into RBS $[\text{Fe}_4\text{S}_3(\text{NO})_7]^-$ and the subsequent reduced-form RBS²⁻ $[\text{Fe}_4\text{S}_3(\text{NO})_7]^{2-}$. The reduced-form $[\text{1Fe-0S}]$ rubredoxin $[\text{Fe}(\text{S-cys})_4]^{2-}$ then triggers trans-nitrosylation of RBS/RBS²⁻, and the sequential insertion/oxidative addition of S derived from S-donor species results in the formation of the preassembled cluster $[\text{Fe}_4\text{S}_4(\text{NO})_4]^{2-}$. The $[\text{Fe}_4\text{S}_4(\text{NO})_4]^{2-}$ cluster can be captured by the $[\text{Fe}(\text{S}_{\text{cys}})_4]^-$ -containing holoprotein to yield $[\text{Fe}_4\text{S}_4]$ -cluster-binding protein, as shown in Scheme 3. The $[\text{Fe}_4\text{S}_4]$ -cluster-binding protein was then delivered to apo-protein to complete the cycle of the degradation and reassembly of the NO-modified $[\text{Fe-S}]$ clusters (Scheme 3).^{6,7} On the basis of this study, IscA protein, proposed to exist as a rubredoxin-containing protein,²³ not only triggers the NO–cysteinate exchange reaction but also delivers the assembled $[\text{Fe}_4\text{S}_4]$ cluster to apo- $[\text{Fe-S}]$ proteins under nitrosative stress-damaged conditions.²⁴ Also, DNICs

- (23) (a) Ding, H.; Clark, R. J. *Biochem. J.* **2004**, *379*, 433–440. (b) Ding, H.; Clark, R. J.; Ding, B. *J. Biol. Chem.* **2004**, *279*, 37499–37504.
 (24) (a) Krebs, C.; Agar, J. N.; Smith, A. D.; Frazzton, J.; Dean, D. R.; Huynh, B. H.; Johnson, M. K. *Biochemistry* **2001**, *40*, 14069–14080. (b) Wollenberg, M.; Berndt, C.; Bill, E.; Schwenn, J. D.; Seidler, A. *Eur. J. Biochem.* **2003**, *270*, 1662–1671.

function not only as NO storage and transporter but also as a nitrosative stress-damaged “descendant”, the precursor of [Fe-S] clusters.

Experimental Section

Manipulations, reactions, and transfers were conducted under nitrogen according to Schlenk techniques or in a glovebox (N₂ gas). Solvents were distilled under nitrogen from appropriate drying agents (diethyl ether from CaH₂; acetonitrile from CaH₂-P₂O₅; methylene chloride from CaH₂; methanol from Mg/I₂; hexane and tetrahydrofuran (THF) from sodium benzophenone) and stored in dried, N₂-filled flasks over 4 Å molecular sieves. Nitrogen was purged through these solvents (including dimethyl formamide (DMF)) before use. Solvent was transferred to the reaction vessel via stainless steel cannula under positive pressure of N₂. The reagents ferric trichloride (Aldrich), elemental sulfur (Showa), sodium (Nihon Seiyaku Industries), bis(triphenylphosphoranylidene)ammonium chloride, and 18-crown-6-ether (TCI) were used as received. Complexes [cation][(NO)₂Fe(SR)₂] (R = Et, Ph),^{17,20} [cation]₂[Fe(SPh)₄],^{15c} and [cation][Fe(SPh)₄] (cation = Na-18-crown-6-ether) were synthesized and characterized by published literatures.^{15c} Infrared spectra of the ν_{NO} stretching frequencies were recorded on a Perkin-Elmer model Spectrum One B spectrometer with sealed solution cells (0.1 mm, CaF₂ windows). UV-vis spectra were recorded on a Jasco V-570 spectrometer. ¹H NMR spectra were obtained on a Varian Unity-500 spectrometer. Analyses of carbon, hydrogen, and nitrogen were obtained with a CHN analyzer (Heraeus).

Preparation of [Na-18-crown-6-ether][Fe(SR)₄] (R = Et, Ph). FeCl₃ (0.1625 g, 1 mmol), NaSR (R = Et (0.336 g, 4 mmol), Ph (0.528 g, 4 mmol)), and 18-crown-6-ether (0.264 g, 1 mmol) were dissolved in DMF (10 mL). The reaction mixture was stirred for 30 min under nitrogen at 0 °C and then further stirred for 5 h at ambient temperature. The reaction mixture was then filtered through Celite to remove the insoluble solid, and diethyl ether was added into the filtrate, leading to the precipitation of complex [Na-18-crown-6-ether][Fe(SR)₄] (R = Et (0.299 g, 51%), Ph (0.335 g, 43%)), characterized by UV-vis spectrum (absorption spectrum (DMF) [λ_{max}, nm]: R = Et (353, 488), R = Ph (328, 554)).^{15c}

Preparation of [Na-18-crown-6-ether]₂[Fe(SPh)₄]. A CH₃CN solution (10 mL) of FeCl₂ (0.127 g, 1 mmol), NaSPh (0.607 g, 4.6 mmol), and 18-crown-6-ether (0.528 g, 2 mmol) was stirred for 30 min under nitrogen at ambient temperature. The reaction solution was filtered through Celite to remove the insoluble solid, and diethyl ether was then added into the filtrate, leading to the precipitation of complex [Na-18-crown-6-ether]₂[Fe(SPh)₄] (0.65 g, 61%), characterized by UV-vis spectrum (absorption spectrum (CH₃CN) [λ_{max}, nm]: 337, 390, 1700).^{15c}

Reaction of [Na-18-crown-6-ether]₂[Fe(SR)₄] (R = Et, Ph) and NO_(g). NO_(g) (48 mL (10% NO + 90% N₂), 0.2 mmol) was added into a CH₃CN solution (10 mL) of complex [Na-18-crown-6-ether][Fe(SR)₄] (R = Et (0.059 g, 0.1 mmol), Ph (0.0786 g, 0.1 mmol)) via a gastight syringe at 0 °C. The reaction solution was stirred for 10 min at ambient temperature and then monitored by FTIR. The IR ν_{NO} spectrum, showing two strong absorption bands at 1721 s, 1679 s cm⁻¹ for R = Et and 1743 s, 1697 s cm⁻¹ for R = Ph, was assigned to the formation of complex [Na-18-crown-6-ether][(NO)₂Fe(SR)₂] (R = Et, Ph), respectively. The solution was then dried under vacuum, and the crude semisolid was redissolved in THF. The mixture was filtered through Celite to remove the insoluble solid, and hexane was added into the filtrate, leading to the precipitation of complex [Na-18-crown-6-ether][(NO)₂Fe(SR)₂] (R = Et (0.0423 g, 81%), Ph (0.0513 g, 83%)), characterized by FTIR and UV-vis spectrum.¹⁷

Reaction of [Na-18-crown-6-ether][(NO)₂Fe(SR)₂] (R = Et, Ph) and S₈. Complexes [Na-18-crown-6-ether][(NO)₂Fe(SR)₂] (R = Et (0.525 g, 1 mmol), Ph (0.622 g, 1 mmol)), and sulfur powder S₈ (0.026 g, 1 mmol) were dissolved in THF (10 mL) and stirred

for 30 min under nitrogen at ambient temperature. The reaction was monitored by FTIR. The IR ν_{NO} shifting from 1715 s, 1673 s cm⁻¹ (R = Et); 1737 s, 1693 s cm⁻¹ (R = Ph) to 1738 s, 1696 s cm⁻¹ was assigned to the formation of the known complex [Na-18-crown-6-ether][(NO)₂FeS₅]. Hexane (15 mL) was then added to precipitate the dark green solid [Na-18-crown-6-ether][(NO)₂FeS₅] (yield 0.52 g, 90%), characterized by IR and UV-vis spectrum.¹⁸

Reaction of [Na-18-crown-6-ether][(NO)₂FeS₅] and Fluoroboric Acid. A THF solution (10 mL) of fluoroboric acid (17.8 μL, 1 mmol) was added dropwise by cannula into a THF solution (5 mL) of [Na-18-crown-6-ether][(NO)₂FeS₅] (0.578 g, 1 mmol), and the mixture solution was then stirred overnight under nitrogen at ambient temperature. The reaction was monitored by FTIR. The IR ν_{NO} shifting from 1738 s, 1696 s cm⁻¹ to 1790 w, 1740 s, 1707 m cm⁻¹ was consistent with the formation of complex [Na-18-crown-6-ether][Fe₄S₃(NO)₇] (**1**).¹⁹ The mixture solution was filtered through Celite to remove the insoluble solid, and hexane was then added to precipitate the dark brown solid complex **1** (0.1491 g, 73%), characterized by IR and UV-vis spectrum.¹⁹

Reaction of [cation][Fe₄S₃(NO)₇] (cation = Na-18-crown-6-ether (1**), Me₄N (1-Me₄N)) and [Na-18-crown-6-ether]₂[Fe(SPh)₄].** To a CH₃CN solution (5 mL) of complex [Na-18-crown-6-ether]₂[Fe(SPh)₄] (0.1599 g, 0.15 mmol) was added in a dropwise manner a CH₃CN solution (5 mL) of complex **1** (0.0817 g, 0.1 mmol) at ambient temperature.¹⁵ The reaction solution was stirred overnight at room temperature and monitored by FTIR. The IR ν_{NO} shifting from 1800 w, 1747 s, 1707 w cm⁻¹ to 1743 s, 1708 s, 1697 sh cm⁻¹ implicated the formation of the known [Na-18-crown-6-ether][(NO)₂Fe(SPh)₂] (1743 s, 1697 s cm⁻¹) and the proposed intermediate [Na-18-crown-6-ether]₂[Fe₄S₃(SPh)(NO)₄] (1708 s cm⁻¹). The mixture solution was then added into a CH₃CN solution of sulfur powder S₈ (0.0032 g, 0.0125 mmol) via cannula under positive N₂ pressure at ambient temperature. After the reaction solution was stirred at ambient temperature for 24 h, the IR ν_{NO} spectrum shifted from 1743 s, 1708 s, 1697 sh cm⁻¹ to 1743 s, 1697 s, 1660 m cm⁻¹, suggesting the formation of [Na-18-crown-6-ether][(NO)₂Fe(SPh)₂] and [Na-18-crown-6-ether]₂[Fe₄S₄(NO)₄] (**3**) (absorption spectrum (CH₃CN) [λ_{max}, nm (ε, M⁻¹ cm⁻¹): 239 (30 405), 263 (21 374), 293 (10 663)].^{20,22} Hexane was added to the mixture solution, extracting the byproduct (PhS)₂, identified by ¹H NMR. The red-brown CH₃CN mixture solution was then filtered through Celite to remove the insoluble solid, and diethyl ether was added into the filtrate to separate the black precipitate complex **3** (0.057 g, 54%), characterized by IR, UV-vis, and single-crystal X-ray diffraction, and the red-brown upper solution. The red-brown upper solution was dried under vacuum and then redissolved in THF-diethyl ether (1:1 volume ratio). The red-brown solution was then filtered through Celite again to remove [Na-18-crown-6-ether][SPh], identified by ¹H NMR, and addition of hexane into the filtrate led to the precipitation of the known [Na-18-crown-6-ether][(NO)₂Fe(SPh)₂] (0.083 g, 89%), characterized by FTIR and UV-vis spectrum.²⁰ In a similar fashion, reaction of complex **1-Me₄N** and [Na-18-crown-6-ether]₂[Fe(SPh)₄], followed by addition of S₈, led to the formation of complex **3-Me₄N**. Recrystallization from a CH₃CN solution of [Me₄N]₂[Fe₄S₄(NO)₄] (**3-Me₄N**) layered with diethyl ether at -20 °C for 2 weeks led to dark crystals suitable for X-ray crystallography.

Reaction of [Na-18-crown-6-ether][Fe₄S₃(NO)₇] (1**) and [Na][biphenyl].** THF solution (5 mL) of sodium metal (0.023 g, 1 mmol) and biphenyl (0.019 g, 0.12 mmol) was stirred under nitrogen for 2 h at room temperature. The purple sodium-biphenyl mixture was then added into a THF solution (5 mL) of complex **1** (0.0817 g, 0.1 mmol) and 18-crown-6-ether (0.0264 g, 0.1 mmol) in a dropwise manner at ambient temperature. After the reaction solution was stirred for 12 h, solvent was removed under positive nitrogen atmosphere to leave the black precipitation. THF was then added to wash the precipitation twice, and the solid was dried under vacuum to yield the black complex [Na-18-crown-6-

ether]₂[Fe₄S₃(NO)₇] (**2**) (0.071 g, 64%), characterized by IR (1748 w, 1690 s, 1660 sh cm⁻¹ (CH₃CN)) and UV-vis spectrum.²¹

Reaction of Complex [Na-18-crown-6-ether]₂[Fe₄S₃(NO)₇] (2**) and [Na-18-crown-6-ether]₂[Fe(SPh)₄].** To a CH₃CN solution (5 mL) of complex [Na-18-crown-6-ether]₂[Fe(SPh)₄] (0.1599 g, 0.15 mmol) was added in a dropwise manner the CH₃CN solution (5 mL) of complex **2** (0.1104 g, 0.1 mmol) at ambient temperature. The reaction solution was stirred at room temperature for 3 h, and the IR ν_{NO} shifting from 1748 w, 1690 s, 1660 sh cm⁻¹ to 1743 s, 1708 s, 1697 sh cm⁻¹ implicated the formation of the known [Na-18-crown-6-ether][(NO)₂Fe(SPh)₂] (1743 s, 1697 s cm⁻¹) and the proposed intermediate [Na-18-crown-6-ether]₂[Fe₄S₃(SPh)(NO)₄] (1708 s cm⁻¹). Then the mixture solution was added into a CH₃CN solution of sulfur powder (0.0032 g, 0.0125 mmol) via cannula under positive N₂ pressure at ambient temperature. After the reaction solution was stirred overnight, the IR ν_{NO} spectrum shifted from 1743 s, 1708 s, 1697 sh cm⁻¹ to 1743 s, 1697 sh, 1660 m cm⁻¹, implicating the formation of the known [Na-18-crown-6-ether][(NO)₂Fe(SPh)₂] and complex **3**.^{20,22} Hexane was added to the mixture to extract the byproduct (PhS)₂, identified by ¹H NMR. The red-brown CH₃CN solution was filtered through Celite to remove the insoluble solid, and then diethyl ether was added into the filtrate to separate the black precipitate complex **3** (0.0516 g, 49%) and the red-brown upper solution. The red-brown upper solution was dried under vacuum and then redissolved in THF-diethyl ether. This red-brown solution was then filtered through Celite to remove [Na-18-crown-6-ether][SPh], and then addition of hexane into the filtrate resulted in the precipitation of the known [Na-18-crown-6-ether][(NO)₂Fe(SPh)₂] (0.072 g, 77%), characterized by IR and UV-vis spectrum.²⁰

Reaction of [Na-18-crown-6-ether]₂[Fe₄S₄(NO)₄] (3**) and [Na-18-crown-6-ether][Fe(SPh)₄].** To a CH₃CN solution (5 mL) of complex [Na-18-crown-6-ether]₂[Fe₄S₄(NO)₄] (0.1046 g, 0.1 mmol) was added in a dropwise manner a CH₃CN solution (5 mL) of [Na-18-crown-6-ether][Fe(SPh)₄] (0.1558 g, 0.2 mmol) at ambient temperature. After the reaction solution was stirred for 10 min at ambient temperature, the IR ν_{NO} shifted from 1660 s cm⁻¹ to 1743 s, 1697 s cm⁻¹, implicating the formation of the known [Na-18-crown-6-ether][(NO)₂Fe(SPh)₂]. The red-brown solution was filtered through Celite to remove the insoluble solid, and then diethyl

ether was added into the filtrate to separate the black precipitate [Na-18-crown-6-ether]₂[Fe₄S₄(SPh)₄] (0.0617 g, 45%), identified by UV-vis and ¹H NMR,¹⁵ and the red-brown upper solution. The filtrate (the red-brown upper solution) was dried under vacuum and then redissolved in THF-diethyl ether. The red-brown solution was then filtered through Celite, and addition of hexane into the filtrate led to the precipitation of black solid [Na-18-crown-6-ether][(NO)₂Fe(SPh)₂] (0.091 g, 73%), characterized by FTIR and UV-vis.²⁰

Crystallography. Crystallographic data and structure refinement parameters of complex [Me₄N]₂[Fe₄S₄(NO)₄] is summarized in the Supporting Information. The crystal chosen for X-ray diffraction studies measured 0.14 × 0.1 × 0.02 mm for complex [Me₄N]₂[Fe₄S₄(NO)₄]. The crystal was mounted on a glass fiber and quickly coated in epoxy resin. Unit-cell parameters were obtained by least-squares refinement. Diffraction measurements for complex [Me₄N]₂[Fe₄S₄(NO)₄] were carried out on a Kappa CCD diffractometer with graphite-monochromated Mo Kα radiation (λ = 0.7107 Å) and between 2.26° and 25.31° for complex [Me₄N]₂[Fe₄S₄(NO)₄]. Least-squares refinement of the positional and anisotropic thermal parameters of all non-hydrogen atoms and hydrogen atoms were fixed at calculated position and refined as riding modes. A multiscan absorption correction was made. The SHELXTL²⁵ structure refinement program was employed.

Acknowledgment. We gratefully acknowledge financial support from the National Science Council of Taiwan. The authors thank Mr. Ting-Shen Kuo for the single-crystal X-ray structural determination.

Supporting Information Available: X-ray crystallographic files in CIF format for the structure determination of [Me₄N]₂[Fe₄S₄(NO)₄]. This material is available free of charge via the Internet at <http://pubs.acs.org>.

JA806050X

(25) Sheldrick, G. M. *SHELXTL, Program for Crystal Structure Determination*; Siemens Analytical X-ray Instruments Inc.: Madison, WI, 1994.